Observation of Half-Height Magnetization Steps in Sr_2RuO_4

J. Jang,[1] D. G. Ferguson,[1] V. Vakaryuk,[1,2] R. Budakian,[1]* S. B. Chung,[3] P. M. Goldbart,[1] Y. Maeno[4]

Spin-triplet superfluids can support exotic objects, such as half-quantum vortices characterized by the nontrivial winding of the spin structure. We present cantilever magnetometry measurements performed on mesoscopic samples of Sr_2RuO_4, a spin-triplet superconductor. With micrometer-sized annular-shaped samples, we observed transitions between integer fluxoid states as well as a regime characterized by "half-integer transitions"—steps in the magnetization with half the height of the ones we observed between integer fluxoid states. These half-height steps are consistent with the existence of half-quantum vortices in superconducting Sr_2RuO_4.

Most known superconductors are characterized by the spin-singlet pairing of the electrons that constitute the superconducting flow. An exception is Sr_2RuO_4 (SRO), which much like the A-phase of superfluid ^{3}He may exist in the equal-spin pairing (ESP) phase (*1*). This phase has been proposed to host half-quantum vortices (HQVs), which are characterized by the relative winding of the phase of the spin-up and spin-down components of the superfluid order parameter (*2*, *3*). In addition to being of basic scientific interest, HQVs are expected to give rise to zero-energy Majorana quasiparticles (*4*, *5*), which have been suggested as a resource for topological quantum computation (*6*).

The ESP state may be thought of as comprising two weakly interacting condensates, having Cooper-pair spin configurations, $|\uparrow\uparrow\rangle$ and $|\downarrow\downarrow\rangle$, defined with respect to a common (ESP) axis. An HQV corresponds to the winding of the phase of only one of these condensates around a contour that encircles the HQV core, such as $(\Delta\theta_\uparrow, \Delta\theta_\downarrow) = (\pm 2\pi, 0)$ or $(0, \pm 2\pi)$, producing half of the magnetic moment of a conventional, full-quantum vortex (FQV), for which $\Delta\theta_\uparrow = \Delta\theta_\downarrow = \pm 2\pi$. The Meissner response of the superconductor screens charge currents over the length scale of the London penetration depth λ; however, any (charge-neutral) spin currents go unscreened. Consequently, the kinetic energy of an isolated HQV diverges logarithmically with the system size, whereas the kinetic energy of a FQV would remain finite. Hence, a single HQV may not be energetically stable in a macroscopic sample, whereas according to (*7*), a single HQV could be stable in a mesoscopic SRO sample of size comparable with or smaller than λ.

We used cantilever magnetometry to measure the magnetic moment of micrometer-sized SRO samples, with the aim of distinguishing between HQV and FQV states via changes in magnetic moment associated with the entry of single vortices. To facilitate this aim, we have fabricated annular samples by drilling a hole in the center of each particle with a focused ion beam. This geometry yields a discrete family of equilibrium states, in which the order parameter winds around the annulus as it would around a vortex core, but evades complications arising from the vortex core.

For an annular conventional superconductor, the fluxoid Φ', defined via $\Phi' = \Phi + (4\pi/c) \times \oint \lambda^2 \vec{j}_s \cdot d\vec{s} = n\Phi_0$, must be an integer multiple n of the flux quantum $\Phi_0 = hc/2e$ for any path encircling the hole (*8*), where h is Planck's constant, c is the speed of light, and e is the electron charge. Here, $\vec{j}_s$ is the supercurrent density, $\Phi = \oint \vec{A} \cdot d\vec{s}$ is the magnetic flux enclosed by the path, $\vec{A}$ is the vector potential, and $n = \oint \vec{\nabla}\theta \cdot d\vec{s}\,/2\pi$ is the order-parameter winding-number along the path. In the regime in which the wall thickness of the annulus becomes comparable with or smaller than λ, $\vec{j}_s$ will not necessarily vanish in the interior of the annulus; hence, it is the fluxoid and not the flux that is quantized. The quantized winding of the order parameter, however, produces observable effects in the magnetic response of the annulus. In the regime in which the magnetization is piecewise linear in the magnetic field, the supercurrents that flow around the hole produce a magnetic moment $\mu_z = \Delta\mu_z n + \chi_M H_z$, where χ_M is the Meissner susceptibility and H_z is the component of the magnetic field that controls the flux through the hole (Fig. 1). In equilibrium, changes in the fluxoid are associated with transitions in the winding number in single units ($n \rightarrow n + 1$), corresponding to the changes in the magnetic moment in increments of $\Delta\mu_z$.

For an ESP superconductor, the two condensates bring the two integer-valued winding numbers: $n_\uparrow$ and $n_\downarrow$. Then, the role of n is played by the half-sum $n = (n_\uparrow + n_\downarrow)/2$. The integer-fluxoid (IF) state of the annulus—the coreless analog of the FQV state—corresponds to the common winding of the condensates ($n_\uparrow = n_\downarrow$), whereas the half-fluxoid (HF) state—the coreless

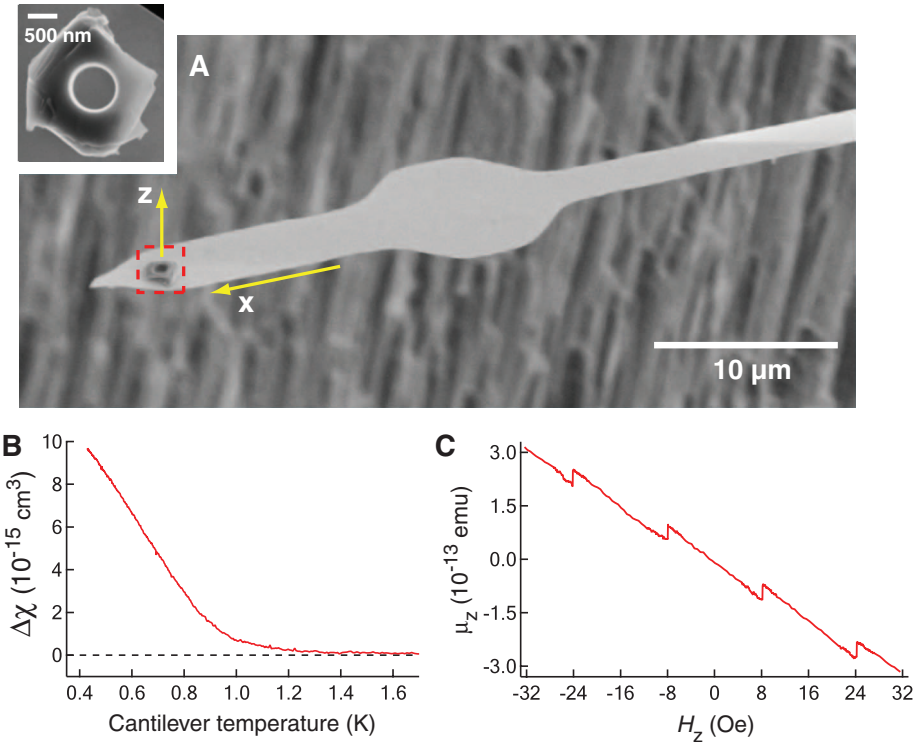

Fig. 1. Image of cantilever with attached annular SRO particle. (**A**) The 80 μm by 3 μm by 100 nm single-crystal silicon cantilever has natural frequency $\omega_0/2\pi = 16$ kHz, spring constant $k = 3.6 \times 10^{-4}$ N/m, and quality factor $Q = 65{,}000$ and exhibits a thermal-limited force sensitivity of $S_F^{1/2} \approx 1.0 \times 10^{-18}$ N/$\sqrt{Hz}$ at $T = 0.5$ K. (Inset) Scanning electron microscopy of the 1.5 μm by 1.8 μm by 0.35 μm annular SRO sample attached to the cantilever. The orientation of the *ab* planes is clearly visible from the layering observed near the edges of the SRO particle. (**B**) Anisotropic component of the susceptibility $\Delta\chi = \chi_c - \chi_{ab}$ as a function of temperature. Here, χ_c and χ_{ab} are the *c* axis and in-plane susceptibilities, respectively. (**C**) Field-cooled data was measured at $T = 0.45$ K for $H_x = 0$.

[1]Department of Physics, University of Illinois at Urbana-Champaign, Urbana, IL 61801–3080, USA. [2]Materials Science Division, Argonne National Laboratory, Argonne, IL 60439, USA. [3]Department of Physics, McCullough Building, Stanford University, Stanford, CA 94305–4045, USA. [4]Department of Physics, Kyoto University, Kyoto 606-8502, Japan.

*To whom correspondence should be addressed. E-mail: budakian@illinois.edu

analog of the HQV state—corresponds to winding numbers that differ by unity ($n_\uparrow = n_\downarrow \pm 1$). Thus, equilibrium transitions between the IF and HF states would change n by half a unit ($n \rightarrow n \pm 1/2$), and this would produce a change $\Delta\mu_z/2$ of the magnetic moment—half of that produced for an equilibrium transition between two IF states (insofar as the corrections produced by nonzero spin polarization are negligible).

To measure the magnetic response of the superconductor, we used a recently developed phase-locked cantilever magnetometry technique (*9*) operating inside a ^{3}He refrigerator with a base temperature of 300 mK (Fig. 1A). In our setup, the displacement of the cantilever was measured by using a fiber optic interferometer operating at a wavelength of 1510 nm. The optical power was maintained at 5 nW in order to minimize heating of the sample from optical absorption. To exclude the potential fortuitous effects of geometry, we present data for three annular SRO particles, of different sizes, fabricated from a high-quality SRO single crystal with a bulk transition temperature T_c = 1.43 K, grown using the floating-zone method (*10*).

We start with the particle shown in Fig. 1A. To characterize its equilibrium fluxoid state, the particle is heated above T_c by momentarily increasing the laser power and then cooled below T_c in the presence of a static magnetic field (field cooling). The field-cooled data (Fig. 1C) exhibits periodic steps in the magnetic moment of nearly constant magnitude $\Delta\mu_z = (4.4 \pm 0.1) \times 10^{-14}$ electromagnetic units (emu), period ΔH_z = (16.1 ± 0.1) Oe, and susceptibility $\chi_M = -6.0 \times 10^{-15}$ cm^3. The measured period ΔH_z is in reasonable agreement with theoretical estimates for the equilibrium fluxoid transitions of a hollow superconducting cylinder having the dimensions of the SRO sample (estimated value of $\Delta H_z \approx 20$ Oe) (*11*). Thus, we conclude that the periodic events observed in Fig. 1C correspond to equilibrium transitions between IF states of the annular SRO particle.

The presence of an in-plane magnetic field H_x brings two new features: (i) For $H_z = 0$, the in-plane magnetic response of the sample exhibits a Meissner behavior for $H_x < 250$ Oe. At $H_x = 250$ Oe, we observed a step in the in-plane magnetic moment with magnitude $\Delta\mu_x \approx 2 \times 10^{-14}$ emu; both the magnitude of the step and the value of H_x at which it occurs are consistent with those expected for the critical field $H_{c1} \parallel ab$ and $\Delta\mu_{ab}$ of an in-plane vortex for our micrometer-sized sample (fig. S3). (ii) For $H_x < H_{c1} \parallel ab$, where no in-plane vortices are expected to penetrate the sample, and in the presence of H_z, we observed the appearance of half-integer (HI) states, for which the change in the magnetic moment of the particle is half that of the IF states.

Figure 2A shows data taken at T = 0.6 K for in-plane fields H_x ranging from –200 to 200 Oe. The data in Fig. 2A were obtained by cooling the sample through T_c in zero field and performing a cyclic field sweep starting at $H_z = 0$ (zero-field cooling). At this temperature, the zero-field cooled and field cooled data are nearly identical, indicating that the equilibrium response is well-described by the zero-field cooled data. Figure 2B shows the data after subtracting the Meissner response; Fig. 2C shows a histogram of the data in Fig. 2B. The steps, which remain, indicate that the change in magnetic moment associated with HI → IF transitions is half of that associated with transitions between two IF states (Table 1). Shown in fig. S4 are zero-field cooled data taken at T = 0.5 K for a direction of the in-plane field having been rotated by 35° in the *ab* plane of the sample. The half-step features remain, and furthermore, the range of H_z values for which the HI state is the equilibrium state is influenced by the magnitude but not the direction of the in-plane field.

To verify that the HI features we observed correspond to fluxoid states and not tilted or kinked vortex lines that pierced the sample walls, we performed an additional series of measurements on a particular SRO annulus in order to determine the dependence of the HI state on the sample geometry. Before each of these measurements, we cut away more of the annulus, using the focused ion beam. The motivation for this study was the following: The location and stability of a vortex line passing through the bulk of the sample should be sensitive to the sample geometry (such as the thickness of the walls of the annulus or the location of pinning sites). In contrast, if the currents responsible for the half-step features are generated by a HI fluxoid—and thus

Table 1. The calculated fractional step heights for the data shown in Fig. 2C. The average value of a given fractional step is indicated by the quantity ⟨…⟩.

H_x (Oe)	$\Delta_1/(\Delta_1 + \Delta_2)$	$\Delta_3/(\Delta_3 + \Delta_4)$
200	0.46 ± 0.06	0.46 ± 0.06
140	0.47 ± 0.05	0.47 ± 0.05
80	0.48 ± 0.06	0.51 ± 0.04
–80	0.45 ± 0.06	0.53 ± 0.09
–140	0.52 ± 0.07	0.51 ± 0.06
–200	0.46 ± 0.07	0.43 ± 0.07
	$\langle\Delta_1/(\Delta_1 + \Delta_2)\rangle$	$\langle\Delta_3/(\Delta_3 + \Delta_4)\rangle$
	0.47 ± 0.03	0.48 ± 0.03

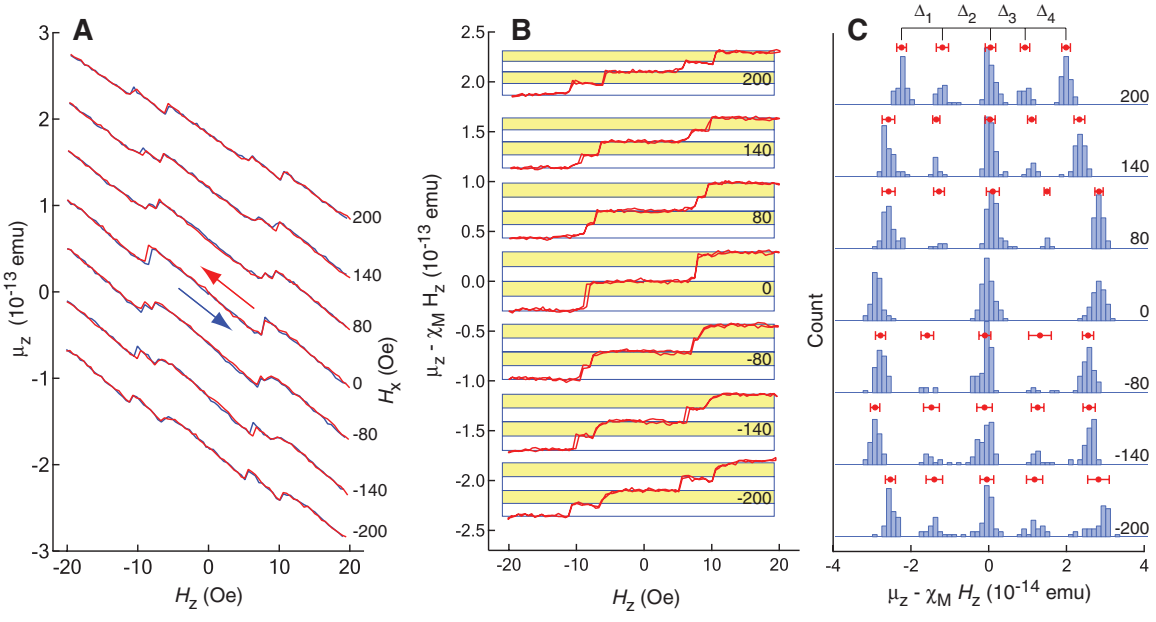

Fig. 2. Evolution of the HI state with in-plane magnetic field. (**A**) Zero-field cooled data obtained at T = 0.6 K. (**B**) Data shown in (A) after subtracting the linear Meissner response; curves have been offset for clarity. (**C**) Histogram of the Meissner-subtracted data. The red points show the mean value of each cluster in the histogram, corresponding to the mean value of a given plateau; the horizontal error bars represent the SD of a given cluster. The change in moment corresponding to the *i*th transition is labeled Δ_i.

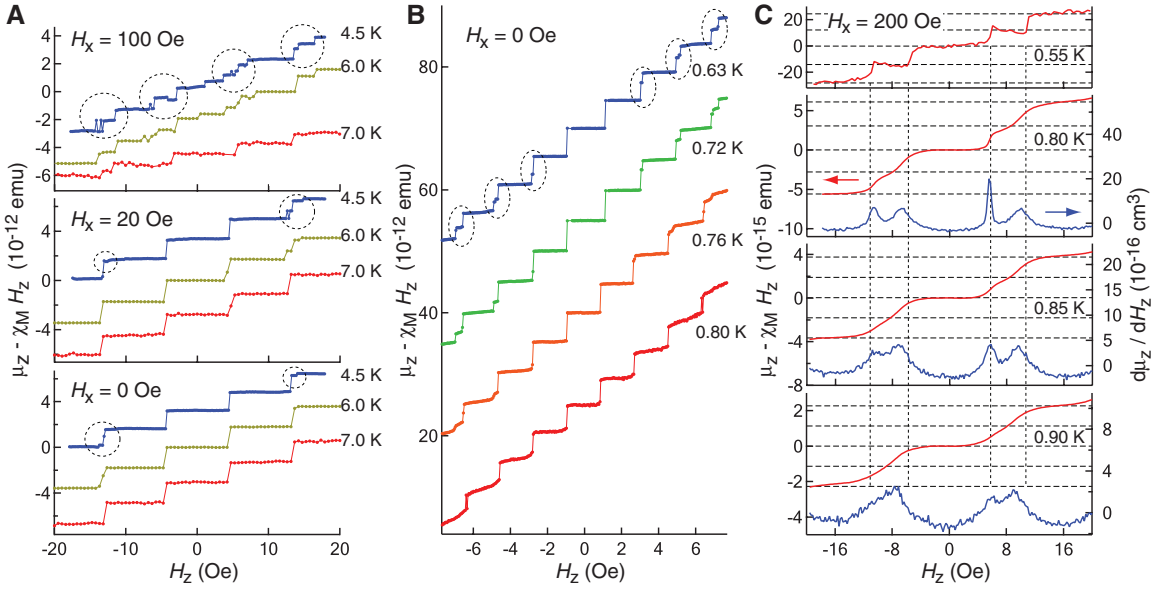

Fig. 3. Temperature evolution of the fractional and HI states. The data were acquired at the value of the in-plane field indicated on the top left-hand corner of each panel; all data were measured by field-cooling the samples. The Meissner response has been subtracted from all data; curves have been offset for clarity. (**A**) Data obtained for the $NbSe_2$ sample (fig. S10). The data are scaled by 4.5 K, 1.0×; 6.0 K, 1.7×; and 7.0 K, 10×. (**B**) Data obtained for the large SRO sample (fig. S9). The data are scaled by 0.63 K, 1.0×; 0.72 K, 1.5×; 0.76 K, 2.3×; and 0.80 K, 6.0×. (**C**) Data obtained for the SRO sample in Fig. 1. The $T = 0.55$ K data are a plot of the c axis moment acquired by applying the phase-locked modulation of $\delta H_x = 1.0$ Oe perpendicular to the c axis. For the $T \geq 0.80$ K data, we measured $d\mu_z/dH_z$ by applying the phase-locked modulation ($\delta H_z = 0.25$ Oe) parallel to the c axis (*9*). The magnetic moment curves are calculated by integrating the measured derivative signal.

only circulate the hole—the observed fractions should not be affected by the sample dimensions. Measurements on a second SRO annulus are shown in fig. S7; the in-plane magnetic field stabilizes an HI state in which the observed fraction is very nearly a half (0.50 ± 0.02). Shown in fig. S8B is the image of the sample presented in fig. S7 (black outline) as well as the outline after reshaping (purple outline). After reshaping, the sample volume was reduced to 44% of the original volume; however, the HI fraction was not affected (0.50 ± 0.01). Half-height step features observed in these samples are robust and not sensitive to the wall thickness or the shape of the boundary.

We have also studied annular samples for which the HI state is not expected to occur: (i) an SRO particle whose dimensions are considerably larger than λ (fig. S9) and (ii) a micrometer-sized particle fabricated from $NbSe_2$—a spin-singlet, layered superconductor (fig. S10). For both of these samples, as the applied field is increased a complicated set of fractional steps in the magnetic moment emerges; their fraction need not be one-half, and it changes with field. Furthermore, the pattern of fractional steps depends on the direction of the in-plane field (changes when $H_x \rightarrow -H_x$). The irregular pattern of fractional steps found for these particles is consistent with the presence of vortices in the bulk of the sample.

The temperature dependence of the fractional steps measured for the large SRO (Fig. 3A) and $NbSe_2$ (Fig. 3B) samples show qualitatively different behavior from that of the HI steps observed for the smaller SRO sample, shown in Fig. 1 (Fig. 3C). As the temperature is raised toward T_c, the fractional steps observed in Fig. 3, A and B, become less pronounced, and most eventually disappear, leaving only the periodic fluxoid transitions. Numerical simulations for thin superconducting discs containing a circular hole (*12*) show that as λ and the coherence length ξ become comparable with or larger than the wall thickness of the ring, the fluxoid states become favored energetically over bulk vortices (vortices penetrating the walls of the superconductor). Thus, at higher temperatures bulk vortices should be less stable—in part because near T_c, ξ and λ will increase and eventually become large (relative to the wall thickness) and also because of increased thermal fluctuations. This behavior is consistent with the temperature dependence observed for the large SRO and $NbSe_2$ samples. In contrast, the HI transitions persist at higher temperature, and the relative contribution to the magnetic moment from each HI transition does not change appreciably with temperature. The HI transitions measured for the SRO sample shown in Fig. 1 exhibit a qualitatively similar temperature dependence to the fluxoid transitions: Near T_c, the HI transitions become reversible and broaden (Fig. 3C), indicating that ξ is comparable with the wall thickness in a portion of the ring. The HI transitions are clearly identified by the two double peaks in the derivative signal.

The HI states observed in magnetometry measurements performed on mesoscopic rings of SRO are consistent with the existence of half-quantum fluxoid states in this system. Our key findings—the reproducibility of the half-height steps in the c axis magnetic moment in multiple samples and their evolution with the applied magnetic field—demonstrate that the HI states are intrinsic to the small SRO annuli. These findings can be understood qualitatively on the basis of existing theoretical models of HQVs [supporting online material (SOM) text]. In addition to the magnetic response, further studies will probe characteristics that are particular to the HQV state, such as spin currents or vortices obeying non-abelian statistics (*13*, *14*).

References and Notes

1. A. P. Mackenzie, Y. Maeno, *Rev. Mod. Phys.* **75**, 657 (2003).
2. G. E. Volovik, V. P. Mineev, *JETP Lett.* **24**, 561 (1976).
3. M. C. Cross, W. F. Brinkman, *J. Low Temp. Phys.* **27**, 683 (1977).
4. N. B. Kopnin, M. M. Salomaa, *Phys. Rev. B* **44**, 9667 (1991).
5. N. Read, D. Green, *Phys. Rev. B* **61**, 10267 (2000).
6. A. Y. Kitaev, *Ann. Phys.* **303**, 2 (2003).
7. S. B. Chung, H. Bluhm, E.-A. Kim, *Phys. Rev. Lett.* **99**, 197002 (2007).
8. F. London, *Superfluids.* (Dover, New York, ed. 2, 1961).
9. Materials and methods are available as supporting material on *Science* Online.
10. Y. Maeno *et al.*, *Nature* **372**, 532 (1994).
11. R. M. Arutunian, G. F. Zharkov, *J. Low Temp. Phys.* **52**, 409 (1983).
12. B. J. Baelus, F. M. Peeters, V. A. Schweigert, *Phys. Rev. B* **61**, 9734 (2000).
13. D. A. Ivanov, *Phys. Rev. Lett.* **86**, 268 (2001).
14. S. Das Sarma, C. Nayak, S. Tewari, *Phys. Rev. B* **73**, 220502 (2006).

15. We thank D. Van Harlingen, M. Stone, E. Fradkin, E.-A. Kim, and H. Bluhm for valuable discussions and M. Ueda for helpful suggestions regarding the data analysis. In particular, the authors thank A. J. Leggett for his theoretical guidance. This work was supported by the U.S. Department of Energy Office of Basic Sciences, grant DEFG02-07ER46453 through the Frederick Seitz Materials Research Laboratory at the University of Illinois at Urbana Champaign and the grants-in-aid for the Global Centers of Excellence "Next Generation of Physics" programs from the Ministry of Education, Culture, Sports, Science and Technology of Japan.

Supporting Online Material

www.sciencemag.org/cgi/content/full/331/6014/186/DC1
Materials and Methods
SOM Text
Figs. S1 to S10
Tables S1 and S2
References

16 June 2010; accepted 8 December 2010
10.1126/science.1193839